

---

# Bayesian Non Parametric Methods for Spike Detection in Calcium Imaging Data

---

Sara Capozio, Daniel Robin  
Université Paris-Dauphine

## 1 Introduction

The paper proposed by Laura d'Angelo, Antonio Canale, Zhaoxia Yu and Michele Guindani, presents the application of nested Bayesian nonparametric models to measure neuronal response to different external stimuli in animals through the analysis of calcium signals. One of the techniques used in biometrics for analyzing neuronal activity is calcium imaging, a method used to record variations in calcium concentration within cells. This methodology involves the use of fluorescent probes that act as sensitive indicators to the presence of calcium. When neurons are activated and calcium floods into the cell generating concentration spikes, the fluorescent probes change their emission state producing a fluorescence trace. Analyzing this trace allows researchers to monitor neuronal activity in real-time and identify which neurons are active in response to which stimuli. It is important to emphasize that we are working with a highly imprecise variable. The fluorescence trace in calcium imaging, while valuable for monitoring neuronal activity, does not perfectly represent the trend of calcium concentration for several reasons. Firstly, the relationship between fluorescence and calcium is nonlinear, leading to a response that is not proportional to the variation in calcium concentration. Additionally, the complex dynamics of binding and release of fluorescent probes can cause delays in fluorescence response compared to actual calcium variations. Therefore, it is important to interpret this variable cautiously and consider its limitations and possible distortions. This analysis was conducted on a publicly available dataset from the Allen Brain Observatory on physiological activity in the mouse visual cortex in response to a series of visual stimuli. Each mouse is placed in front of a screen where different types of visual stimuli are shown, while neuronal activity is recorded. The aim of the study is to investigate how neurons at different depths in the visual areas respond to stimuli of different complexity through the application of a coherent nested hierarchical Bayesian finite mixture model. This model allows for the estimation of spike activity of each neuron and the reconstruction of spike distributions under various experimental conditions. In this report, we will review the main ideas of the proposed model, show you some initial results and explore an attempt of improvement of the model.

## 1 Priors and Hypothesis

Let us first explain how the model was built from a probabilistic perspective. The temporal behavior of the fluorescence trace is modeled through the definition of two main equations:

1) The observation and measurement equation:

$$y_t = b + c_t + \epsilon_t$$

where:

- $b$ : represents the baseline level of brain activity
- $c_t$ : the level of calcium concentration at time  $t$
- $\epsilon_t \sim N(0, \sigma^2)$  the noise

2) The transition equation that models the calcium level through a first-order auto-regressive model

$$c_t = \gamma c_{t-1} + A_t + \omega_t$$

38 where:  
 39 –  $\gamma$  is the auto-regressive coefficient which controls the natural decay of calcium concentration.  
 40 Assuming that the time series is stationary, we constrain this parameter to be in  $]0; 1[$   
 41 –  $c_{t-1}$ : calcium level at time  $t - 1$   
 42 –  $A_t$ : indicates the spike intensity at time  $t$ . When a spike occurs, the concentration increases with  
 43 respect to the intensity of the neuronal activation.  
 44 –  $\omega_t \sim N(0, \tau^2)$ : is the noise in calcium concentration

45 Overall, the fluorescence trace follows a normal distribution:

$$y_t \sim N(b + \gamma c_{t-1} + A_t, \sigma^2 + \tau^2)$$

46 with the following fixed priors on the unknown parameters and with arbitrarily fixed hyper-parameters:

47  
 48 –  $\frac{1}{\sigma^2} \sim \text{Gamma}(h_{1\sigma}, h_{2\sigma})$ .  
 49 –  $b \sim N(b_0, B_0)$   
 50 –  $c_0 \sim N(0, C_0)$   
 51 –  $\gamma \sim \text{Beta}(h_{1\gamma}, h_{2\gamma})$   
 52 –  $\frac{1}{\tau^2} \sim \text{Gamma}(h_{1\tau}, h_{2\tau})$

53 It is known that neuronal activity can vary significantly in response to different experimental stimuli.  
 54 The fundamental objective is therefore to create a hierarchical model that allows us to examine how  
 55 neuronal activity is distributed across different scenarios. In practice, we want to group experimental  
 56 data into clusters to identify if certain scenarios exhibit similar patterns of neuronal activity. The main  
 57 objective of the analysis is therefore to infer the level of spike intensity  $A_t$ . Let  $J$  be the total number  
 58 of settings considered, and let  $g_t$  be a discrete categorical variable taking values from  $\{1, \dots, J\}$ ,  
 59 indicating which scenario each recorded neuronal activity at time  $t$  belongs to. It is assumed that the  
 60 spikes  $A_t$  follow stimulus-specific distributions. Each type of stimulus elicits a different neuronal  
 61 response modeled by the distribution  $G_j$ :  $A_t | g_t = j \sim G_j$

62 Despite the presence of various stimuli, some scenarios may exhibit similar patterns of neuronal  
 63 activity. This means that over the  $J$  settings, we expect only  $K$  different clusters of neuronal behaviors  
 64 (with  $K < J$ ). The main objective is to cluster the probability distributions  $G_1, \dots, G_J$  in order to  
 65 identify similar patterns of neuronal activity across different experimental conditions. We model it as  
 66 a general mixture of mixtures :

$$G_1, \dots, G_J | Q \sim Q, \quad Q = \sum_{k=1}^K \pi_k \delta_{G_k^*}$$

67 where:

68 –  $\pi_1, \dots, \pi_K \sim \text{Dirichlet}_K\left(\frac{a}{K}, \dots, \frac{a}{K}\right)$  , with  $a > 0$   
 69 –  $K$ (number of clusters)  $\sim \text{Beta\_negative\_binomial}$   
 70 –  $G_1^*, \dots, G_K^*$  are the realizations of a finite mixture model.

71 For every behavioral cluster, the neuronal activity is characterized by different spikes intensities  
 72 that may be shared by different settings. For instance there could be a level of "strong intensity  
 73 neuronal activity" that is reached with probability  $q_1$  in behavioral cluster 1 and with probability  $q_5$   
 74 in behavioral cluster 5. To represent this aspect, we will define a set of spike intensities  $A_1^*, \dots, A_L^*$   
 75 on which the behavioral clusters' distributions will take support. Mathematically,

$$G_k^* = \sum_{l=1}^L \omega_{l,k} \delta_{A_l^*}$$

76 where

77 –  $(\omega_{1,k}, \dots, \omega_{L,k}) \sim \text{Dirichlet}_L\left(\frac{\beta}{L}, \dots, \frac{\beta}{L}\right)$  , with  $\beta > 0$ .  
 78 –  $A_l^* \sim G_0 = (1 - p)\delta_0 + p \cdot \text{Gamma}(h_{A1}, h_{A2})$  , a spike and slab mixture prior. We will carefully  
 79 choose the parameters of the gamma distribution as we want to make sure we clearly separate the  
 80 points with no activity from the spikes with an intensity adequately far from 0.  
 81 –  $p$  (proportion of spikes)  $\sim \text{Beta}(h_{1p}, h_{2p})$ , with  $h_{1p} \ll h_{2p}$ .

82 As a result we obtain a model where every setting is linked to a behavioral cluster of neuronal activity.  
 83 Each behavioral cluster defines a distribution on neuronal activity spikes. Moreover these spikes of  
 84 activity are shared by the clusters, thus representing different levels of activation a neuron can hit.

## 85 2 Posterior Inference

### 86 2.0.1 The method

87 Once the model has been defined, the authors suggest a method to find the posterior distribution of  
88 the parameters of the model. This interests us as we want to reproduce the whole underlying activity.  
89 The method mixes several statistical and Monte Carlo Markov Chains techniques such as Gibb's  
90 sampling, Kalman filtering and nested telescopic sampling. The entire sampling procedure used in  
91 the coding phase is reported below:

92 1. Kalman Filter: the calcium level  $c_t$  is sampled using a Kalman filter and a forward filtering  
93 backward sampling method. The Kalman filter provides a recursive estimate of the state variable  
94 based on the previous state estimate and the current observation, while taking into account the system  
95 dynamics and measurement noise.

96 2. The parameter  $b$  is sampled through Gibb's sampling step. The posterior distribution of the baseline  
97 level is given by  $b \sim N(\frac{b_0}{B_0} + \frac{1}{\sigma^2} \sum_{t=1}^T (y_t - c_t), \sqrt{\frac{1}{B_0} + \frac{T}{\sigma^2}})$

98 3. Similarly we use a single Gibb's sampling step for the parameters  $\sigma$  and  $\tau$ . The posterior  
99 distributions for the two parameters are respectively

100  $\frac{1}{\sigma^2} \sim \text{Gamma}(h_{1\sigma} + \frac{T}{2}, h_{2\sigma} + \frac{1}{2} \sum_{t=1}^T (y_t - c_t - b)^2)$

101  $\frac{1}{\tau^2} \sim \text{Gamma}(h_{1\tau} + \frac{T}{2}, h_{2\tau} + \frac{1}{2} \sum_{t=1}^T (c_t - \gamma c_{t-1} - A_t)^2).$

102 4. The parameter  $\gamma$  is sampled through a Metropolis-Hastings. At each iteration a new value of  
103 gamma is proposed and accepted with respect to the Metropolis-Hastings ratio.

104 5. The weight of the Dirichlet processes and the clusters allocating variables are sampled through a  
105 nested telescopic sampling.

106 6. Finally we use a Gibb's sampling step to sample a new parameter  $p \sim \text{Beta}(h_{1p} + T - n_0, h_{2p} + n_0)$ ,  
107 where  $n_0$  is the number of time stamps where  $A_t = 0$ .

108 At the end of this process, we have updated one time the whole model. After a few burn-in steps, we  
109 should start getting values approximately following the real posterior distribution of the model.

### 110 2.0.2 The results

111 The procedure described above was applied to the Allen Brain Observatory mouse brain data. The  
112 data represent the fluorescent trace detected by exposing a sample of mice to three different stimuli:  
113 static gratings, natural scene and natural movie. The number of scenario taken into account is  $J=4$ ,  
114 with level 4 representing the category: 'absence of stimuli'. The clustering model reveals a similarity  
115 in the distribution of neural activity across the mouse exposed to natural scene and natural movies.  
116 However, for the category static grating, the distribution of spikes appeared to differ significantly. To  
117 analyze the spike variation across scenarios, a metric called firing rate was computed. This indicator  
118 measures how often the neurons activate during a specific visual stimulus calculating the number of  
119 detected spike per second. For the static grating stimulus the average posterior firing rate takes a value  
120 equal to 0.223, while the others two categories it takes a value equal to 0.419 and 0.511 respectively.  
121 In conclusion, it was demonstrated that there exists an association between neural activity and the  
122 complexity of the stimuli.

## 123 3 Extensions

### 124 3.0.1 Sensitivity analysis

125 The sensitivity analysis was conducted to assess how variations in the input values of the model affect  
126 the model's outcomes. Essentially, the main objective is to understand how sensitive the model's  
127 responses are to changes in its parameters or initial conditions. This approach aims to identify the  
128 most sensitive parameters and to define their range of variability. The hyper-parameters we focused  
129 on are those related to the definition of the spike and slab priors. One of the key points of the paper is  
130 to assign specific distributions to parameters  $A_t$  (intensity of the spikes) and  $p$  (proportion of spikes)

in order to enforce sparsity in the detection of spikes. The authors chose priors for these parameters capable of inducing a clear separation between baseline neuronal activity and neuronal response:

$$A_t^* \sim G_0 = (1 - p)\delta_0 + p \cdot \text{Gamma}(h_{A1}, h_{A2})$$

$$p \text{ (proportion of spikes)} \sim \text{Beta}(h_{1p}, h_{2p})$$

The choice of hyper-parameter values is crucial to enforce the sparsity, indeed the higher the shape parameter  $h_{A1}$  and the smaller  $h_{1p}$  is with respect to  $h_{2p}$ , the larger is the separation. During the analysis, the authors fixed the following values for the hyper-parameters:  $h_{A1}=8$ ,  $h_{A2}=8$ ,  $h_{1p}=1$ ,  $h_{2p}=999$ . Through a simulation approach, we analyzed the robustness of the model by assessing how the posterior distribution changed as these parameters varied. Firstly, focusing on  $p$ , it was found that as the hyper-parameters changed, the posterior distribution for  $A_t$  remained very stable.

The inference made on this parameter appears to be highly robust to changes in the hyper-parameters. On the contrary, the inference made on the spike intensity values appears to be much more sensitive. Keeping the scale parameter constant, we analyzed the behavior of the posterior distribution of intensities as the shape parameter varied. After several simulations, it was noticed that the shape of the posterior distribution of  $A_t$  seemed to be highly variable when higher scale parameters (greater than 16) were chosen.

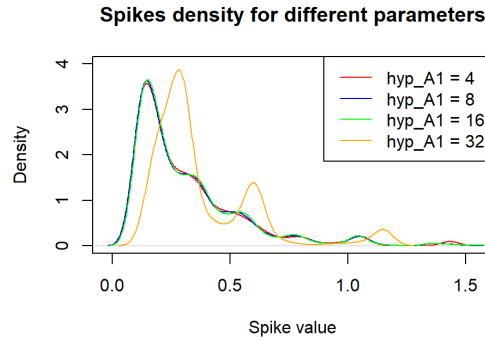


Figure 1: Param 1A

Since during the model validation phase, the empirical average intensities assumed a value of 1.5, it was decided to maintain scale and shape parameters consistent with the real-world results. For this reason, it is appropriate to consider shape parameter values between 8 and 16. Since in this range of variation, the specific choice of the hyper-parameter does not seem to have a significant impact on the posterior distribution, we can conclude that the inference made on  $A_t$  is robust.

### 3.0.2 Time dependency of the spikes

The authors applied the model without assuming a particular auto-correlation structure for the intensities  $A_t$ . This could represent an unrealistic scenario as typically spike intensities might exhibit an underlying auto-correlation structure that describes how the series evolves over time. For this reason a possible extension to this model is adding a time dependence on the values of the  $A_t$ . In order to check the robustness of our model against time-correlated spikes we tested its performances on a set of simulated data under the assumption that they follow an auto-regressive process. To model this auto correlation we did as follows. At every time  $t$ , if there was a spike at the previous time step, we increased the probability (by a fixed value  $\rho$ ) of having a nonzero spike. In this way, we have constructed a temporal dependency between spike levels that tends to exponentially decay as the time window increases. We assessed the performance of the model checking the value of the Rand Index in Distributional estimation (attributing each spike to the right cluster of distribution), and on Observational estimation (predicting the value of each spike intensity). As we can see by comparing the original scenario and the time-dependent one, the results are very close, with a decrease of performance and an increased variability in the time-dependent case. So the introduction of time-correlated data slightly weakens the model. Yet the model still achieves very good predictions.

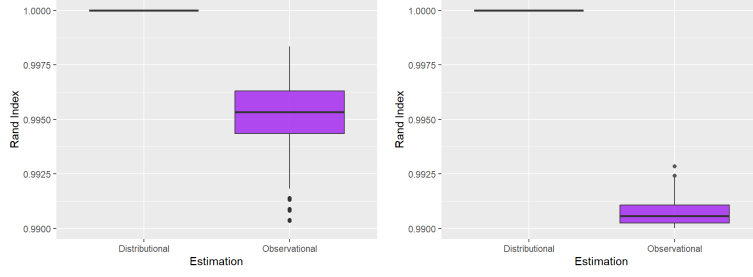


Figure 2: Rand Indexes of our simulations. On the left, the classical setting. On the right, simulation with time-dependent spike intensities

168 It is interesting to note that, as showed in the auto correlation plots, the model successfully catches  
 169 the time dependence structure of the spike intensities, despite the absence of time correlated structure  
 170 in its priors.

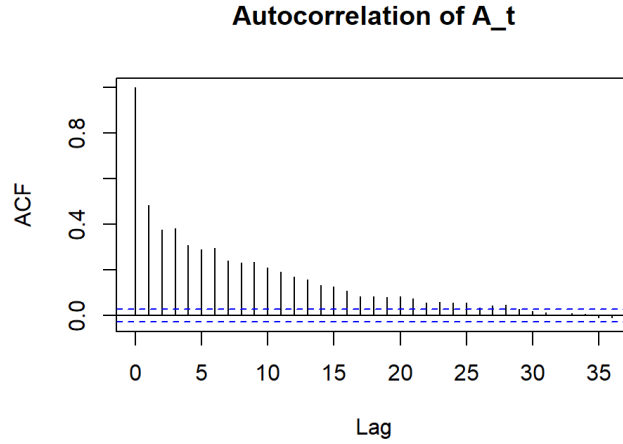


Figure 3: Autocorrelation plot of the posterior estimated spikes, for simulated data with time-dependency with  $\rho=0.5$

171 The main reason why the model appears to work under the assumption of auto-correlation among the  
 172 data might be related to the fact that during the posterior inference, this property is preserved thanks  
 173 to the strong information content of the sample. At the end, different scenarios belonging to the same  
 174 cluster will exhibit the same distribution of spike intensities while sharing the same auto-correlation  
 175 structure.

## 176 Conclusion

177 In conclusion, this report aimed to revisit the application of a hierarchical nested Bayesian model  
 178 to reconstruct spike distributions under various experimental conditions from both theoretical and  
 179 empirical perspectives. Through the application of sensitivity analysis, we assessed the robustness of  
 180 the method with respect to the hyper-parameters used in the spike and slab priors, obtaining satisfying  
 181 results. Then we explored a potential extension of the model, through the addition of time dependent  
 182 auto-correlation of the spike intensities. We found that the model was robust to this type of structure  
 183 in the empirical data as it was able to reproduce in the posterior inference the auto-correlation property  
 184 of the spike intensities. Overall this study highlights the strength of this model in different situations,  
 185 as no flaw was proven.